DNA Damage by Thiol-Activated Neocarzinostatin Chromophore at Bulged Sites†

Feng Gu, Zhen Xi, and Irving H. Goldberg*

Department of Biological Chemistry and Molecular Pharmacology, Harvard Medical School, Boston, Massachusetts 02115

Received January 4, 2000; Revised Manuscript Received February 17, 2000

ABSTRACT: Bulge structures in nucleic acids are of general biological significance and are potential targets for therapeutic drugs. It has been shown in a previous study that thiol-activated neocarzinostatin chromophore is able to cleave duplex DNA selectively at a position opposite a single unpaired cytosine or thymine base on the 3′ side. In this work, we studied in greater detail the nature of this type of cleavage and the basis for the selectivity of the bulge site cleavage over the usual strand cleavage at a T site in the duplex region by using duplexes containing an internal control and a bulge, which is composed of different types and number of bases. Experimental results indicated that the bulge-induced cleavage is initiated by 5′ hydrogen abstraction and is greatly affected by the base composition of the bulge. A single-base bulge, especially when containing a purine, yields higher efficiency and greater selectivity for the bulge-induced cleavage. In particular, a single adenine base gives rise to the highest cleavage yield and provides over 20 times greater selectivity for cleavage at the bulge site compared with the internal control site in duplexes. The binding dissociation constants of postactivated drug for a stem-loop structure containing a one- or two-base bulge in the stem, measured by fluorescence quenching, show that the binding is about 3−4 times stronger for bulge-containing duplexes than for perfect hairpin duplexes. For RNA·DNA hybrid duplexes, where the DNA is the target strand and the RNA is the bulge-containing strand, bulge-induced cleavage was observed, although at low yield. On the other hand, when RNA is the nonbulge strand, no bulge-induced cleavage was found. When the reaction is performed in the absence of oxygen, the major product is a covalent adduct, and it is at the same location as the cleavage site under aerobic conditions.

Neocarzinostatin (NCS), the first member of the enediyne antitumor family of antibiotics to be discovered, has been subjected to extensive mechanistic study (see refs *1*−*4*). It is generally accepted that the nonprotein chromophore of this antibiotic (NCS-chrom, **1**) is responsible for its DNA cleavage activity and that its naphthoate ester moiety intercalates via the minor groove of the DNA duplex, allowing the epoxybicyclo-[7,3,0]-dodecadiendiyne portion of the chromophore to be positioned in the minor groove (*5*). Activation by a thiol generates a cumulene intermediate capable of undergoing a Bergman-type rearrangement into a diradical species (*6*), which can abstract a hydrogen atom from the 5′, 1′, or 4′ carbons of the deoxyribose of DNA to form carbon-centered radicals at these positions (Scheme 1). Under aerobic conditions, the carbon radicals are oxidized, leading to strand scissions or abasic sites as final DNA damage products. NCS-chrom has exhibited both base-specific single-strand (ss) and sequence-specific double-strand (ds) cleavages. Many of the lesions result from single-strand cleavage, mostly caused by C-5′ hydrogen abstraction from thymidine or deoxyadenosine residues. This kind of abstraction leads to the formation of nucleoside 5′ aldehyde and 3′ phosphate fragments as the final products. Double-strand (ds) cleavage occurs with AGC- or AGT-containing sequences, where both the C-2 and C-6 radical centers of the drug abstract hydrogens from the two complementary DNA strands simultaneously (*2*). To account for the ds cleavage, the three-dimensional NMR structure of a complex formed between a postactivated drug and an AGC containing duplex has been elucidated (*7*, *8*).

Scheme 1: Proposed Activation and DNA Damage Mechanisms of NCS−Chrom by Thiol

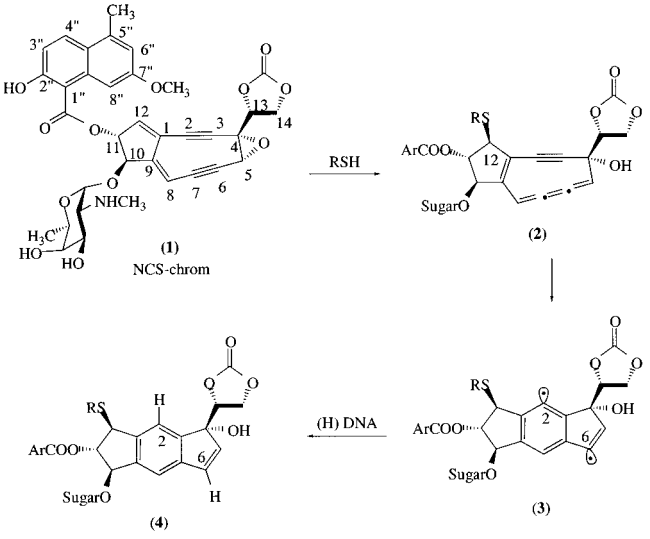

Significantly, NCS-chrom has recently been found to undergo other activation pathways to DNA-reactive species besides that involving thiol (see ref *1*). It has been shown that, under neutral or basic conditions, in the absence of thiol,

† This work was supported by U.S. Public Health Service Grant GM 53793 from the NIH.

* To whom correspondence should be addressed. Phone: (617) 432-1787. Fax: (617) 432-0471. E-mail: irving_goldberg@hms.harvard.edu.

10.1021/bi000007t CCC: $19.00
Published on Web 03/30/2000

duplex DNA containing a two-base bulge can be effectively cleaved by NCS-chrom (*9*, *10*). The cleavage is restricted to a nucleotide in the bulge, at its 3′ side, and is entirely due to an initial 5′ hydrogen abstraction. This reaction was rationalized by a mechanism involving a general base-catalyzed intramolecular Michael addition, resulting in a spirolactone cumulene intermediate, which further generates a 2,6-didehydroindacene biradical, responsible for the hydrogen abstraction from the sugar chain at the bulge site (*11*). The cleavage is bulge specific, and regular duplex DNAs or DNAs containing a single unpaired base are not cleaved under similar conditions. The solution structure of the complex formed between the wedge-shaped isostructural form of the active spirolactone diradical species and a DNA oligonucleotide containing a two-base bulge was elucidated by NMR spectroscopy (*12*). From this structure, it is clear that the reactive drug species binds via the major groove to the triangular prism pocket formed by the two looped-out bases and the neighboring base pairs, with which the two drug rings of the wedge-shaped molecule stack. Most recently, a detailed mechanistic study of the roles of bulged DNA in the base-catalyzed transformation of NCS-chrom was performed (*13*).

Bulge structures in nucleic acids, involving one or more unpaired bases, are of general biological significance (*14*, *15*). Bulges are very common among RNAs, and they play important roles in protein binding recognition (*16*). On the other hand, DNA bulges are believed to be involved in frameshift mutation (*17*, *18*) and are the products of imperfect homologous recombination or slipped mispairing during the replication of DNA (*19*). DNA bulges have been shown to be targets for DNA repair enzymes (*20*, *21*). Multibase bulges, such as triplet repeats, have been implicated in inherited neurodegenerative diseases such as Huntington's disease (*22* and references therein). Consequently, nucleic acid bulges have been the subject of intense recent study. The local conformations of single-base bulges in several DNA oligonucleotides have been characterized by NMR spectroscopy (*23*, *24*). It has been found that the equilibrium between a nucleotide bulge intercalating in or looping out of the helix depends on the temperature, the identity of the bulge nucleotide, and the sequence of base pairs in the duplex surrounding the bulges (*23*, *25*). Single purine bases are prone to intercalate into the helix, while pyrimidine bases can be either in or out of the helix. Thermodynamic exploration indicates that, for single-base bulges, pyrimidine bases are on average ~0.5 kcal mol^{-1} more stable than purine bases (*26*). Bulges can cause kinks (*14*) and bending (*27*) in the DNA helix, and it has been shown that DNA intercalators, such as ethidium, much prefer bulged regions over normal duplex regions (*28*−*30*).

Williams and Goldberg studied the recognition of a single cytosine or thymine base bulge by several DNA intercalating and cleaving agents, including thiol-activated NCS-chrom (*31*, *32*). It was found that the latter causes specific scission on the strand opposite to the unpaired base at the position just 3′ to the bulge site, whereas on the bulge-containing strand, the single-strand cleavage at the T site nearest to the bulge is diminished. In as much as single-base bulge sites are potential drug targets, a detailed analysis of this reaction appears to be a worthwhile undertaking. We show here that the preference for cleavage at a single-base bulge site over that at a single-strand cleavage site in the duplex region is greatly affected by the type and number of bulge-containing bases. We also provide data showing that the bulge-induced cleavage is due to an initial 5′ hydrogen abstraction. Moreover, when the reaction is performed under anaerobic conditions, a covalent DNA adduct is formed at the aerobic cleavage site on the strand opposite the bulge. Further, binding studies show that preferred cleavage across from the bulge involves kinetic factors in addition to enhanced binding at the site.

MATERIAL AND METHODS

Nucleoside phosphoramidites, solvents, and reagents for DNA and RNA synthesis were purchased from Glen Research. T4 polynucleotide kinase and T4 RNA ligase were obtained from New England Biolabs. Terminal deoxynucleotidyl transferase was from Pharmacia Biotech. [γ-^{32}P]ATP, [5′-^{32}P]pCp, and [α-^{32}P]cordycepin triphosphate were from New England Nuclear-Dupont. Fifteen or twenty percent denaturing polyacrylamide gels were prepared with Sequagel stock from National Diagnostics. Gel electrophoresis was performed in a 1× TBE buffer (GIBCO BRL) at room temperature and 800−1500 V. Nondenaturing polyacrylamide gels were prepared with ProtoGel stock of National Diagnostics and the electrophoresis was carried out at 400 V in a 4 °C cold room. All other reagents and chemicals were from Aldrich, Sigma, Fisher Scientific, or other chemical distributors. NCS was purchased from Kayaku Antibiotics (Japan). NCS-chrom was extracted with MeOH and stored at −80 °C in the dark, as described previously (*33*).

DNA Oligonucleotide Preparation and Labeling. All DNA and RNA oligonucleotides were synthesized by the standard β-cyanoethyl phosphoramidite method on an ABI 381A DNA synthesizer. DNAs were deprotected by treating with concentrated aqueous ammonia at 50 °C for 16 h and desalted through Bio-Rad Econo-Pac 10 DG chromatography columns. RNAs were deprotected by first reacting with 2 M ammonia in methanol at 50 °C for 15 h and then treating the dried supernant with tetrabutylammonium fluoride at room temperature for 10 h to remove the silyl protection group from the 2′-positions. The oligos were desalted and used directly or further purified by 15 or 20% polyacrylamide gel (PAGE), if necessary. The 5′ ends of oligonucleotide were labeled with [γ-^{32}P]ATP and T4 polynucleotide kinase. The 3′ ends were either labeled with [5′-^{32}P]pCp and T4 RNA ligase (for RNA) or [α-^{32}P]cordycepin triphosphate and terminal transferase (for DNA). The labeled oligonucleotides were purified on a 15% gel, and the appropriate bands were excised, crushed, and soaked with sterile water and desalted with G-25 Sephadex columns.

Reactions of the Duplexed DNA (RNA) with Drug. Oligonucleotides containing 5′ or 3′ end-labeled sequences were annealed with their complementary strands in a Tris-HCl buffer by heating at 90 °C for 2 min and slowly cooled to room temperature. Glutathione solution was then added. The vials containing annealed duplexes were placed in ice, and the reaction was initiated by adding the drug solution in cold methanol into the vials in the dark. After mixing, the mixture was allowed to stand in the ice in dark for 1 h. A typical reaction was carried out in a volume of 20 μL of

aqueous solution containing 40 mM Tris·HCl (pH 8.5), 1 mM EDTA, <10% v/v methanol, 12.5 μM duplexed DNA (RNA), 5 mM glutathione, and 15 μM drug. The pH of the final reaction mixture was 7.5. After the reaction, the samples were dried in a SpeedVac concentrator, resuspended in loading buffer, and analyzed on 15 or 20% PAGE.

The anaerobic reactions were carried out in a Warburg vessel. The sidearm contained 50 μL of the mixture of GSH and Tris-HCl buffer (pH 8.5), while DNA duplex and drug in NaOAc buffer (pH 5.0, total volume 250 μL) were placed in the main chamber. The contents of the vessel were degassed by a freeze−evacuate−thaw procedure (*34*), and the evacuation was repeated four times to ensure that oxygen is completely removed from the system. The reaction was initiated by mixing the solutions between the sidearm and main chamber at 4 °C with protection from light. The mixed solution was allowed to stand in ice for 1 h. The final concentrations of the components of the solution (total volume 300 μL) were NaOAc, 20 mM; Tris-HCl, 50 mM; thiol, 1 mM; DNA duplex, 12.5 μM; drug, 15 μM; MeOH, 10% (v/v), and pH 8.0. The oligos were then dried and purified on a 20% gel. Bands corresponding to the adduct were excised from the gel and eluted with water by following the crush and soak procedure. The eluant was desalted through G-25 Sephadex columns or Sep-Pack columns and Speed-Vac dried or lyophilized for sequencing analysis.

Chemical Sequencing and Reactions. For DNA oligonucleotides, the C + T reaction was carried out in 100 mM hydrazine at 37 °C for 30 min and the oligomers were subsequently precipitated with cold ethanol at −20 °C. Formic acid was used for the A + G reaction, and 1.2 M NaOH/EDTA solution was used for the A > C reaction, as described previously (*35*). After precipitation with cold ethanol, all the precipitates were subjected to alkaline treatment as described below. RNAs was treated with 0.2 M Na_2HPO_4 at 50 °C for 1 h.

Alkaline treatment was performed by heating the samples in 100 μL of 1 M piperidine at 90 °C for 30 min. The piperidine was removed by coevaporating with water three times using Speed-Vac. $NaBH_4$ treatment was carried out in 0.2 M $NaBH_4$ for 2 h at room temperature. Borane hydride treatment was carried out in 80 mM BH_3/pyridine aqueous solution by addition of 1 M BH_3/pyridine complex in 2-propanol, and the mixture was incubated at room temperature for 20 h. Oxidation of the 5′ aldehyde fragment was performed by treating the samples with NaOI by adding the mixture of 0.1 M KI_3 and 0.5 M Na_2CO_3 (pH 9.0) into the vial containing the sample. The mixture was allowed to stand at room temperature for 30 min and then neutralized with cold 1 M HCl and treated with 15 mM $Na_2S_2O_3$ to remove the excess amount of the oxidizing agent.

All the radioactive gel bands were quantitated with a Bio-Rad PhosphorImager screen by exposing the screen to the gel in the dark; the screen was then scanned using Bio-Rad Molecular Imager FX. The intensity area integration was performed with Bio-Rad Quantity One software.

Measurement of the Binding Dissociation Constants. Fluorescence quenching studies were carried out with a SPEX Fluoro Max-2 at 0 °C in a 10 mM phosphate buffer (pH 7.5) (*36*). For the measurement, annealed hairpin DNA solutions were gradually added into the buffer containing glutathione post-activated drug, and the fluorescence reading was recorded after an equilibrium had been reached (excitation 360 nm, emission 440 nm). The dissociation constants (K_d) were derived from curve-fitting with Kaleidagraph, using the equation

$$i/i_0 = 1 + (\Delta i/2i_0)([T_0] + [DNA] + K_d)^2 - 4[T_0][DNA])^{1/2}$$

where $[T_0]$ is the initial concentration of the fluorescent probe, i is the intensity of the sample, i_0 is the initial intensity of the sample, [DNA] is the concentration of the DNA, and Δi is the total change in intensity per drug unit from the free state to the total binding state (*36*).

RESULTS AND DISCUSSION

DNA Cleavage Specifically at the Site Opposite to the Bulge: Effect of Type and Number of Bases in the Bulge. Figure 1 lists the oligonucleotides used in these experiments. A 12-mer oligonucleotide 5′-CGACCCAAATGC-3′ (D_1) was chosen as the nonbulge containing target strand. The single T residue is placed in the duplex region as an internal control, since it is expected to be a major single-strand cleavage site, based on previous results. D_{1-0} is a DNA 12-mer that forms a perfect duplex with D_1. All the other strands (D_{1-1} to D_{1-21}) contain an extra base or bases between G(8) and G(9) of the parent strand D_{1-0}. These unpaired bases can form a bulge when each of these strands is annealed with D_1, and the bulge will be located directly opposite the site between C(4) and C(5) of D_1. There are five bases between the internal control target (T residue) and the bulge site of D_1, so that interference between the two sites should be minimal. Up to five pyrimidine residues were inserted at the bulge site (D_{1-1} to D_{1-9}). For purine bases, bulges of one to three adenines (D_{1-10} to D_{1-12}) or one guanine (D_{1-15}) were studied. Three kinds of chemical linkers, which resemble the nucleic acid sugar−phosphate backbone, were also studied as bulge-mimicking components (D_{1-16} to D_{1-20}). Finally, D_{21} is composed of two DNA strands lacking an interconnecting phosphodiester linkage and thus contains a break between G(8) and G(9) at the original bulge site, when annealed with D_1.

D_1 was 5′ end-labeled with ^{32}P and annealed with various complementary strands (D_{1-0} to D_{1-21}). The duplexes formed were reacted with glutathione-activated NCS-chrom, and after the reaction, each of the mixtures was desalted and separated on a 15% denaturing gel. Figure 2 shows typical gel electrophoretic patterns for strand scission of these bulge-containing duplexes by thiol-activated NCS-chorm. As can be seen, the perfect duplex (D_1 with D_{1-0}) has a strong cleavage band at the T site and a moderate band at the A site of the normal duplex (lane 3 in Figure 2A and lane 2 in Figure 2B), which is consistent with previous results (*31*). Cleavage at these sites exists for all the bulge-containing duplexes, although the intensities vary.

There is very strong cleavage across from the bulge structures for almost all the bulge-containing duplexes, which corresponds to the C(5) position of the Maxam−Gilbert sequencing lanes. The bulge formed by a single A base leads to the strongest cleavage on the target strand at the C(5) site. This is not only shown by the highest intensity among the cleavage bands at the same location but by the highest

DNAs:

D_1 5'-CGACCCAAATGC-3'

D_{1-0} - D_{1-20} 3'-GCTG GGTTTACG-5'
X

D_{1-21} 3'-GCTG-5' 3'-GGTTTACG-5'

D_2 5'-CGAGGGAAATGC-3'

D_{2-0} - D_{1-20} 3'-GCTC CCTTTACG-5'
Y

S = L$_9$ = L$_3$ =

RNAs:

R_1 5'-CGACCCAAAUGC-3'
C

R_2 3'-GCUG GGUUUACG-5'
A

R_3 3'-GCUG GGUUUACG-5'

Oligonucleotides

name	bulge bases (X)	name	bulge bases (Y)
D_{1-0}	none	D_{2-0}	none
D_{1-1}	C	D_{2-1}	A
D_{1-2}	CC	D_{2-2}	AA
D_{1-3}	CCC	D_{2-3}	AAA
D_{1-4}	CCCC	D_{2-4}	T
D_{1-5}	CCCCC	D_{2-5}	TT
D_{1-6}	T	D_{2-6}	TTT
D_{1-7}	TT	D_{2-7}	G
D_{1-8}	TTT	D_{2-8}	GG
D_{1-9}	TTTT	D_{2-9}	GGG
D_{1-10}	A	D_{2-10}	C
D_{1-11}	AA		
D_{1-12}	AAA		
D_{1-13}	CA		
D_{1-14}	AC		
D_{1-15}	G		
D_{1-16}	S		
D_{1-17}	SS		
D_{1-18}	L_9		
D_{1-19}	L_3		
D_{1-20}	L_3L_3		
D_{1-21}	strand break		

FIGURE 1: Sequences of oligonucleotides (names in bold). D_1, D_2, and R_3 are nonbulge containing target strands. D_{1-0} and D_{2-0} are perfect complementary strands of D_1 and D_2, respectively. The remaining strands contain extra unpaired base(s) so as to form a bulge in the duplex. D_{1-21} are two strands lacking a connecting phosphodiester linkage so as to form a strand break at the supposed bulge site with D_1.

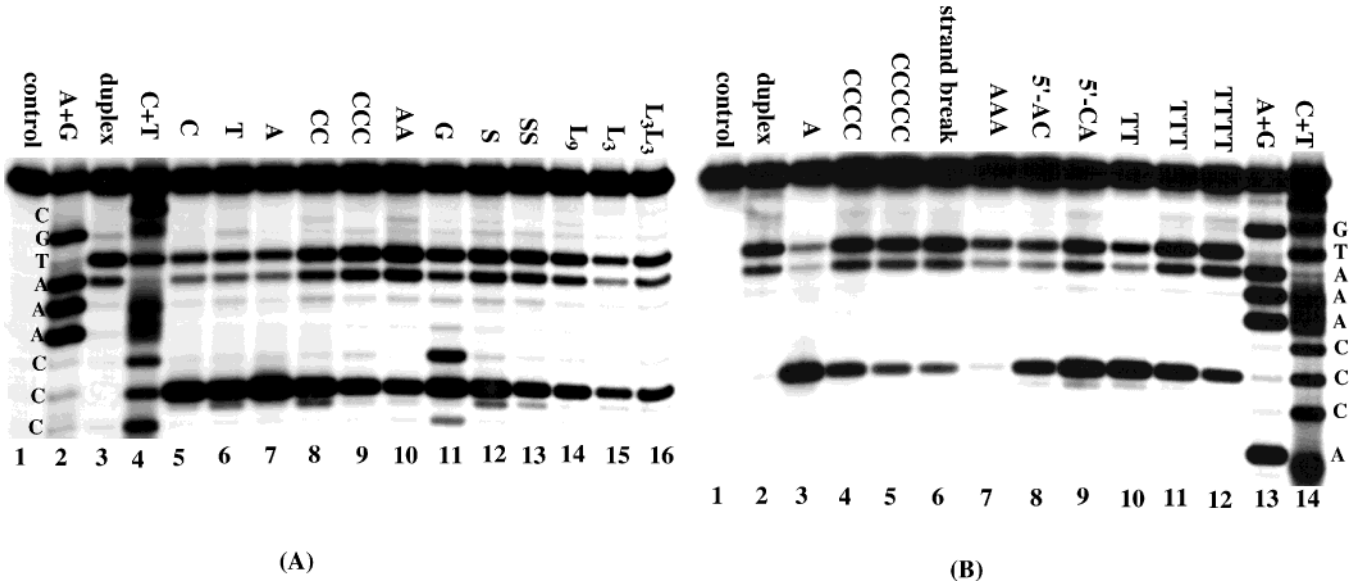

FIGURE 2: DNA cleavage of duplexes containing 5′ end-labeled D_1 with various complementary strands containing an extra base(s) on the bulge strands, as indicated at the top of each lane. (A) lane 1, control without drug; lanes 2 and 4, Maxam−Gilbert chemical sequencing lanes; lane 3, perfect duplex ($D_1 + D_{1-0}$); lanes 6−16, bulge containing duplexes. (B) lane 1, control; lane 2, perfect duplex; lanes 13 and 14, chemical sequencing lanes; lane 6, duplex formed from D_1 and D_{1-21} (containing a strand break instead of a bulge); the remaining lanes, bulge containing duplexes. The area integration value of each band is summarized in Table 1.

selectivity [selectivity Index (SI) = 23; Table 1] when compared with the cleavage at the internal control T (and A) site (lane 7 of Figure 2A and lane 3 of Figure 2B). Table 1 lists the selectivity indices of the bulge-induced cleavages versus the T site cleavages of each lane. Several remarks should be made from these results. (1) At the same drug/substrate ratio, for single-base bulges, cleavage is preferred at the bulge site rather than the internal control site in the duplex region (SI > 10, except for G base, see below), and for two or more base bulges, the SI drops dramatically (selectivity on bulge-induced cleavage over T site cleavage is 5.6-fold for two Cs and 0.3 for five Cs). (2) The cleavage specificity at a single-base bulge is A > C > T ≫ chemical linkers (lanes 7, 11, 5, 6, and 12−16 of Figure 2A). (3) For the A base, the cleavage induced by a two-base bulge is much weaker than by a single base and almost negligible for a three-base bulge (lanes 7 and 3 of Figure 2B and lanes 10 and 7 of Figure 2A). (4) For pyrimidine bases (C and T), two-base bulges lead to cleavage that is about half that of the a single-base ones in terms of selectivity (lanes 5 and 8

Table 1: Bulge-Induced Cleavage on the Target Strand D_1 from Duplexes of D_1 with Bulge Containing Strands[a]

oligo	bulge base	relative cleavage (%)[b]	selectivity index[c]	oligo	bulge base	relative cleavage (%)[b]	selectivity index[c]
D_{1-1}	C	44	11.7	D_{1-13}	AC	15	1.4
D_{1-2}	CC	66	5.6	D_{1-14}	CA	56	2.3
D_{1-3}	CCC	19	1.4	D_{1-15}	G	52	5.7
D_{1-4}	CCCC	15	0.5	D_{1-16}	S	26	2.8
D_{1-5}	CCCCC	7	0.3	D_{1-17}	SS	17	1.5
D_{1-6}	T	35	9.4	D_{1-18}	L_9	10	1.5
D_{1-7}	TT	58	4.6	D_{1-19}	L_3	3	1.2
D_{1-8}	TTT	38	1.0	D_{1-20}	L_3L_3	5	1.2
D_{1-9}	TTTT	11	0.3	D_{1-21}	break	6	0.2
D_{1-10}	A	100	23.5	R_2	RNA C	4.7	−
D_{1-11}	AA	9	0.7	R_3	RNA A	2.1	−
D_{1-12}	AAA	2	0.2				

[a] Names of the oligonucleotides complementary to D_1 as described in Figure 1. [b] Relative percentage values of the bulge-induced cleavages in each duplex (intensity percentage of the cleavage band at the bulge opposite the "C" site in each lane) compared to the A bulge, which is normalized to 100%. [c] Ratio of bulge site cleavage versus the internal control (*T*) site cleavage (intensity ratio of the two bands).

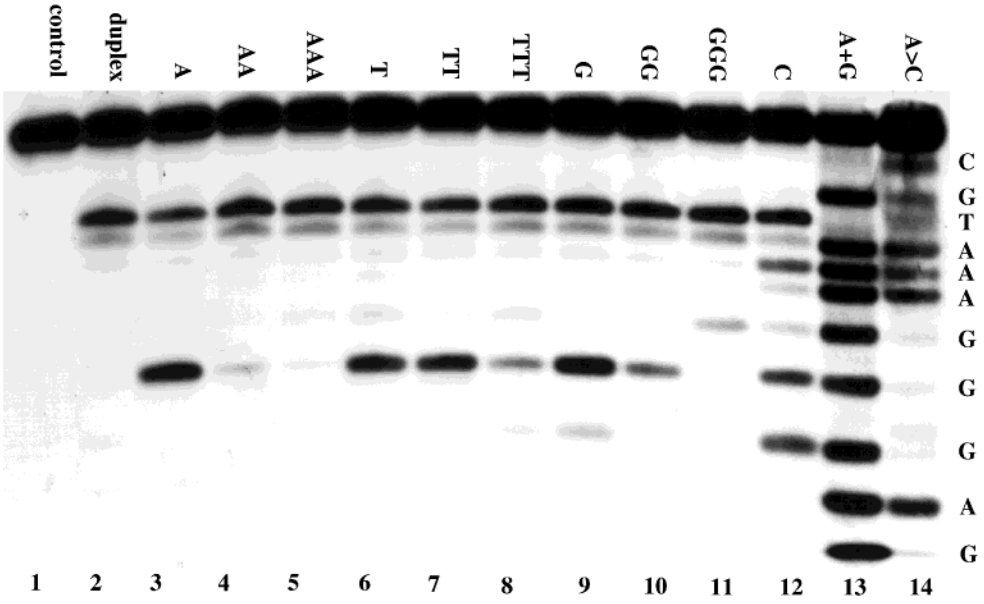

FIGURE 3: DNA cleavage of duplexes containing 5′ end-labeled D_2 with various complementary strands containing an extra base(s) on the bulge strands, as indicated at the top of each lane. Lane 1, control without drug; lanes 2, perfect duplex (D_2 and D_{2-0}); lanes 13 and 14, Maxam−Gilbert chemical sequencing lanes; the remaining lanes, duplexes containing various bulges. The area integration value of each band is summarized in Table 2.

of Figure 2A for C, and lane 6 of Figure 2A and lane 10 of Figure 2B for T), and the cleavage is weaker with three more bases (lane 9 of Figure 2A, lanes 4 and 5 of Figure 2B for C, and lanes 11 and 12 of Figure 2B for T). (5) Cleavage induced by the 5′-CA bulge is almost 4 times that by the 5′-AC bulge (lanes 9 and 8 of Figure 2B), and the SI is also higher for the CA bulge. (6) Because the extra G base at the bulge can cause base slippage in the bulge region, we observe cleavage at all C positions [C(4), C(5), and C(6)], although C(5) is the main cleavage site (lane 11, Figure 2A). Probably because of the slippage, the combined area of the three bands yields a moderate degree of cleavage as compared with other bases. (7) Cleavage data from chemical linkers (D_{1-16} − D_{1-20}) show that one abasic site mimic (D_{1-16}) probably retains a significant structural element of the bulge. A strand break on the complementary strand of D_1 at the supposed bulge location causes moderate cleavage on D_1 (lane 6, Figure 2B), but when there is a gap due to deletion of G(8) on the duplex, there is no obvious induced cleavage (data not shown). This is different from an earlier report showing that dynemicin A induces strand scission at a location adjacent to a one-base gap on the opposite strand (*37*). These results imply that a strong drug interaction with the bulge needs more than just the spacious binding pocket.

To explore whether these results are general for all sequences with thiol-activated NCS-chrom, another group of bulges containing DNA duplexes was tested. As shown in Figure 1, the target strand D_2 has a similar sequence as D_1 except that C(4) to C(6) are replaced by three G bases. The bulge containing complementary strands have their extra base(s) located at the same position as that of the D_1 duplexes, i.e., between C(8) and C(9) of the parent strand D_{2-0}. The reactions were performed in a similar way as for the D_1 duplexes, and the gel results are shown in Figure 3. The bulges induce cleavage on the target strand at the G(5) of D_2, and although the cleavage efficiencies and selectivity indexes are generally lower than that of the D_1 duplexes, which may indicate the importance of the two bases adjacent to the bulge bases on the bulge strand (pyrimidine versus purine bases), they follow a very similar pattern: (1) for

Table 2: Bulge-Induced Cleavage on the Target Strand D_2 from Duplexes of D_2 with Bulge Containing Strands[a]

oligo	bulge base	relative cleavage (%)[b]	selectivity index[c]
D_{2-1}	A	100	3.15
D_{2-2}	AA	10	0.09
D_{2-3}	AAA	2	0.04
D_{2-4}	T	49	1.11
D_{2-5}	TT	45	1.04
D_{2-6}	TTT	15	0.31
D_{2-7}	G	73	1.66
D_{2-8}	GG	6	0.33
D_{2-9}	GGG	0.4	0.06
D_{2-10}	C	58	

[a] Names of the oligonucleotides complementary to D_2 as described in Figure 1. [b] Relative percentage values of the bulge-induced cleavages in each duplex (intensity percentage of the cleavage band at the bulge opposite "C" site in each lane) compared to the A bulge, which is normalized to 100%. [c] Ratio of bulge site cleavage versus the internal control (*T*) site cleavage (intensity ratio of the two bands).

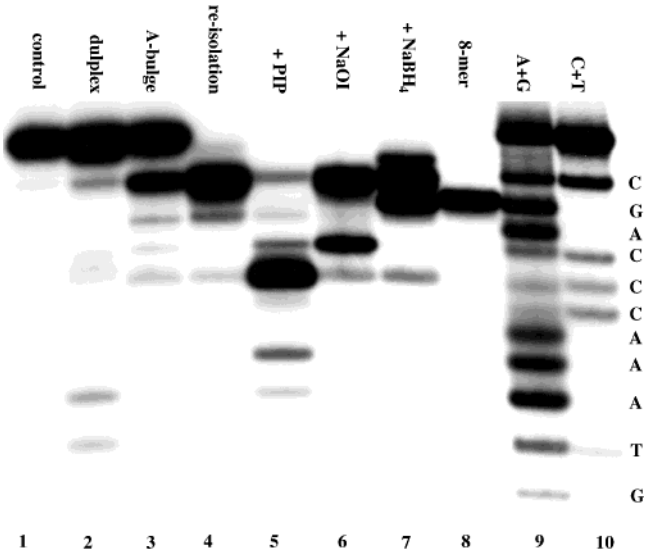

FIGURE 4: Chemical reactions and sequencing of 3′ end-labeled D_1 and related strands in determination of the cleavage chemistry. Lanes 1−3, reaction of D_1 and D_{1-0} or D_{1-10} duplexes with thiol-activated NCS-chrom: lane 1, no drug control; lane 2, D_1 and D_{1-0}; lane 3, D_1 and D_{1-10}, lane 4, reisolation of the 8-mer aldehyde from lane 3; lanes 5−7, chemical treatments of the sample from lane 4; lane 8, 8-mer oligonucleotide synthesized independently (5′-GCATTTGG-^{32}P-3′); lanes 9 and 10, sequencing lanes of 3′ end labeled D_1. Conditions of chemical treatment are as described in Materials and Methods.

single-base bulges, purines (A and G) cause stronger cleavages than the pyrimidine base (T) with a pattern of A > G > T (lanes 3, 9, 6, and 12); (2) for two-base bulges, the drop in selectivity from one base to two or more bases is much less significant for pyrimidine bases (lanes 6−8) than that of purine bases (lanes 3−5 and 9−11) (Table 2). In agreement with earlier results (*31*), there was no cleavage in the bulge region itself when the bulge-containing strands were labeled and examined after the reaction (data not shown).

The observed greater efficiency of cleavage opposite a purine-containing bulge may be due to thermodynamic and/or kinetic factors. Binding studies (vide infra) indicate that kinetic considerations relating to the geometry of the cleavage complex are likely responsible for the difference in cleavage opposite a purine or a pyrimidine-containing bulge. It is striking how a simple bulge can induce such strong, specific DNA damage by thiol-activated NCS-chrom. In light of the NMR structures of the complex formed between thiol postactivated NCS-chrom and duplex DNA (*7*, *8*), which shows a minor groove drug binding mode, and that between alkali-inactivated NCS-chrom and a two-base bulge DNA (*12*), which shows a major groove drug binding mode, the binding mode of the drug−DNA interaction studied here is of particular interest. A preliminary NMR study of a complex from a thiol post-activated NCS-chrom and a DNA hairpin containing a one-base bulge shows similar drug−DNA interaction patterns as observed in the NMR structure of a complex formed between thiol post-activated NCS-chrom and a duplex DNA (*7*, *8*), suggesting naphthoate intercalation occur via the minor groove (X. Gao, Z. Xi, and I. H. Goldberg, unpublished data). The intercalation site appears to be the bulge proper.

Chemistry of DNA Cleavage at Bulged Sites by Thiol-Activated NCS-chrom. It is well established that thiol-activated NCS-chrom can undergo 5′, 1′, and 4′ hydrogen abstractions with various DNA duplexes (see refs *1*−*4*). Among them, single-strand 5′ cleavage at T residues predominates. This kind of damage generates fragments with 5′ nucleoside aldehyde and 3′ phosphate ends (Scheme 2). As shown in Figures 2 and 3, we observed that the bulge-related cleavage bands at the nonbulge strand have the same

Scheme 2: Proposed Mechanism of NCS−Induced DNA Damage at C-5′ Position

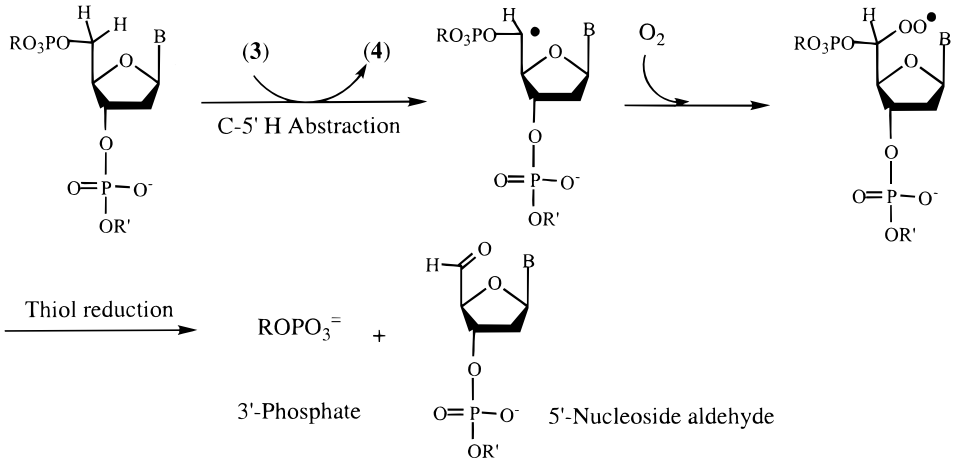

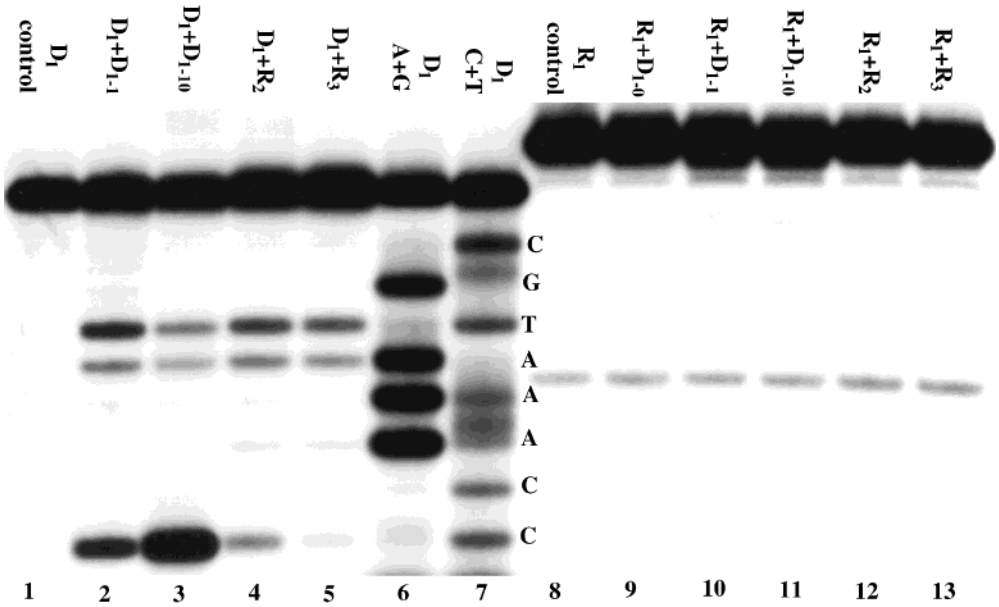

FIGURE 5: Reactions of thiol-activated NCS-chrom with bulge containing duplexes involving RNA strands. Lanes 1−5, 5′ end-labeled D_1 with various complementary strands, as indicated at the top of each lane; lanes 6 and 7, chemical sequencing of D_1; lanes 8−13, 5′ end-labeled R_1 with various complementary strands as indicated; lane 8, control lane without drug.

Table 3: Dissocation Constants and Cleavage Selectivity Indices for Hairpin Duplexes[a]

entry	oligonuclides	dissociation constant (μM)[b]	cleavage selectivity index[c]
1	5′-CGACCCAAATGC-L_9-GCATTTGGGTCG	0.150	n/a
2	5′-CGACCCAAATGC-L_9-GCATTTGG**A**GTCG	0.043	7.9
3	5′-CGACCCAAATGC-L_9-GCATTTGG**AA**GTCG	0.053	0.71
4	5′-CGACCCAAATGC-L_9-GCATTTGG**C**GTCG	0.041	2.7
5	5′-CGACCCAAATGC-L_9-GCATTTGG**CC**GTCG	0.038	2.4
6	5′-CGACCCAAATGC-L_9-GCATTTGG**CCC**GTCG	0.140	n/a
7	5′-CGACCCAAATGC-L_9-GCATTTGG**T**GTCG	0.047	n/a
8	5′-CGACCCAAATGC-L_9-GCATTTGG**TT**GTCG	0.031	n/a

[a] The bulge-containing strand was connected to its otherwise complementary strand by L_9 [L_9 = $O(CH_2CH_2O)_2CH_2CH_2O$-] to form a hairpin-like structure. The bulge bases are shown in bold. [b] Binding dissociation constants (μM) as measured by fluorescence quenching and derived from curve-fitting with Kaleidagraph software (see Materials and Methods). [c] Cleavage selectivity index for bulge-induced cleavage versus that at the internal control site (T_{10}) measured from the reaction of thiol-activated drug with various hairpin duplexes.

mobility as the sequencing bands, indicating that they are 3′ phosphate-ended, suggesting that the cleavage is likely to be due to 5′ chemistry. To obtain further evidence for this, we labeled the target strand at the 3′ terminus with [^{32}P]-cordycepin triphosphate and terminal transferase. The major cleavage band (from the duplex containing an A bulge) was isolated and subjected to subsequent chemical treatments. Figure 4 illustrates the results from these reactions, clearly demonstrating the 5′ chemistry. Thus, the major aldehyde band was converted by piperidine treatment to a fragment with a 5′ phosphate (lane 5), oxidation with NaOI leads to the formation of the 5′ carboxylic acid, which moves more slowly than the phosphate band (one base shorter) (lane 6), and reduction with $NaBH_4$ generates an 8-mer alcohol (lane 7), which has the identical mobility as that of the authentic octamer (lane 8). The products from the reactions and the mobilities of all the bands are characteristic of a 5′ aldehyde fragment, providing further evidence for an initial 5′ hydrogen abstraction for this type of reaction (*9*).

Bulge-Induced Cleavage Involving RNA. In general, duplex RNAs are not good substrates for NCS-induced cleavage (*2*). However, it has been shown that glutathione-activated NCS-chrom generates staggered double-strand lesions in DNA−RNA hybrids (*38*). This type of lesion involves 1′ hydrogen abstraction from the targeted ribonucleotide on the RNA strand and 5′ chemistry on the DNA side. On the other hand, for the general base-catalyzed reactions, NCS-chrom-induced strand cleavage occurs selectively at the bulge of the trans activation region RNA (TAR RNA) of HIV type I, but the efficiency of cleavage was very low (*39*). Since bulges are very common in the secondary structures of RNA, it would be of interest to see if there is any cleavage activity related to the bulges involving RNA oligonucleotides with thiol-activated NCS-chrom. We synthesized three RNA oligomers, which have similar sequences as D_1, D_{1-1}, and D_{1-10} (thymine bases are replaced by uridine bases for RNA, see Figure 1). The cleavage experiments were performed with gluthathione-activated NCS-chrom and annealed bulge-containing DNA-RNA, RNA-DNA hybrids, and RNA-RNA duplexes (Figure 5). Interestingly, when DNA is the target strand and RNA is the bulge side, there is weak cleavage at the usual T and A sites (lanes 4 and 5), and the intensities for these bands are compatible with their DNA counterpart (lanes 2 and 3). On

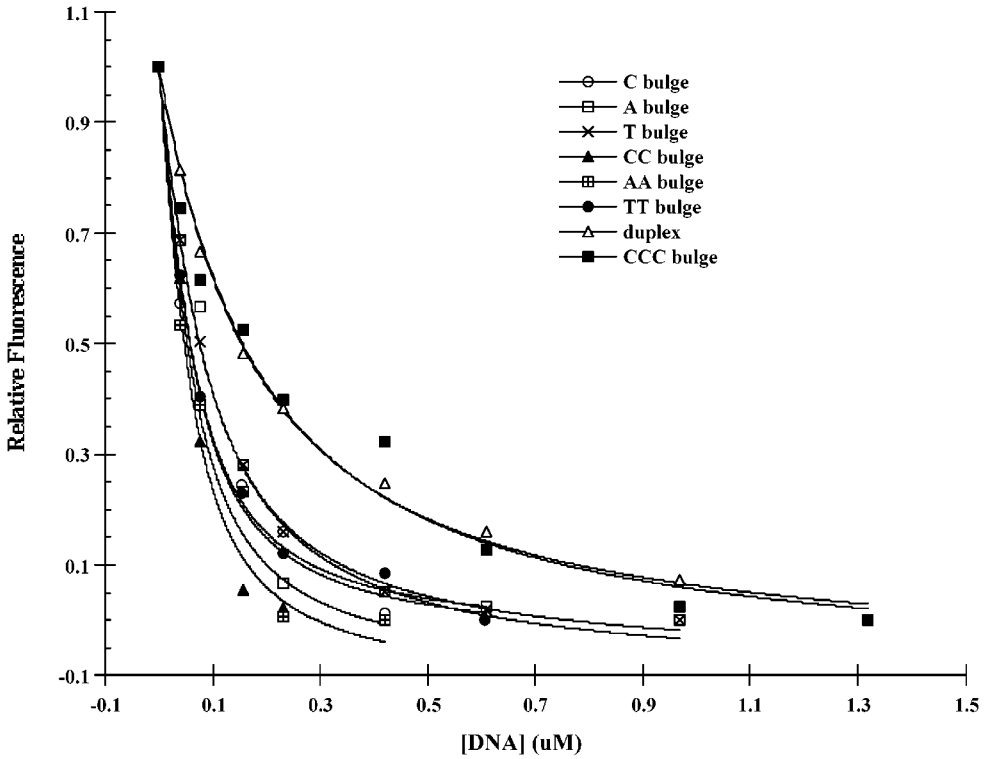

FIGURE 6: Fluorescence quenching of glutathione-activated NCS-chrom by hairpin DNAs. Experimental details are as described in Materials and Methods. The K_d values were calculated by curving fitting for each experiment and are summarized in Table 3. Curve fitting was performed by using Kaleidagraph software.

the other hand, for the bulge-induced cleavages, there is very weak cleavage corresponding to the C(5) position with the RNA C (R_2) bulge, and with the RNA A (R_3) bulge, this is even fainter. This is in contrast to DNA bulges where A > C. The intensity for lesions induced by the RNA C bulge is less than 10% of the one by DNA C bulge.

On the other hand, when RNA is the target strand and the bulge strand is either DNA or RNA, no cleavage was observed (lanes 10−13).

The reason for the dramatic differences between DNA and RNA is still unclear, but it is likely that it is due to the inherent structural and conformational differences between these two types of biopolymers. DNA duplexes prefer B-form as its major conformation in aqueous solution, in which the furanose rings are in C-2′-endo conformation. The furanose ring of RNA has stronger preference for C3′-endo geometry. As a result, RNA duplexes and DNA−RNA hybrids normally adopt the A-form conformation. Clearly, the binding of the drug could be much different for these two forms. Furthermore, the extra 2′-OH group on RNAs could also play a critical role in the binding and/or positioning of the drug at the bulge site for an effective initial hydrogen abstraction. Taken together, these two factors could account for a much weaker cleavage on the DNA strands when they are the target strands in hybrid duplexes and no cleavage at all on the RNA strands in either hybrid or duplex RNAs. In previous studies with the base-catalyzed NCS-chrom cleavage of DNA bulges, substituting the DNA bulge regions with ribonucleotides caused almost a 90% decrease in cleavage efficiency (*40*). The 2′-hydroxyl group of the ribonucleoside was implicated as introducing steric clash with the 7′′-O-methyl moiety of the naphthoate moiety of the chromophore, resulting in much less cleavage. A similar situation could also contribute to the observed cleavage patterns involving RNA reported here.

Binding and Cleavage of Bulge-Containing Hairpin Duplexes. The reported dissociation constants (K_d) for the complex formed between glutathione postactivated NCS-chrom and 7-mer DNA duplexes containing a single binding site are in the range of 2−30 μM (*41*). These measurements were based on the quenching of fluorescence (at 440 nm) of the drug upon DNA binding. Given the fact that bulge-induced cleavage is at least 10 times stronger than that at the internal control site, it was anticipated that the bulge site would also be a much more preferred binding site for the drug.

To ensure that there is efficient duplex formation at low DNA concentrations, the two complementary DNA strands, one of which contained a bulge, were connected by a linker to form a hairpin-like structure. Accordingly, we designed several hairpin DNA strands, which in general are D_1 plus its complementary strands connected by chemical linker L_9 (Table 3). The dissociation constants measured by fluorescence quenching necessarily reflect the availability of multiple competing binding sites on the formed duplex. The binding data at the lowest DNA concentration, however, represent the preferred binding at the strongest binding site (Figure 6). Table 3 gives the K_d values for the tight-binding region, obtained from curve fitting of the data. Interestingly, the K_d values for one- or two-base bulge containing hairpin duplexes are $\leq$0.050 μM. The binding constant for the perfect hairpin duplex is close to 0.15 μM, and the bulge containing three cytosine bases has a similar value. It is significant that the binding of the drug to bulge-containing duplexes having one or two unpaired bases is about 3 times stronger than that to the perfect duplex. Also, the binding does not distinguish between purine or pyrimidine unpaired bases in the bulge. While the adenine base bulge showed

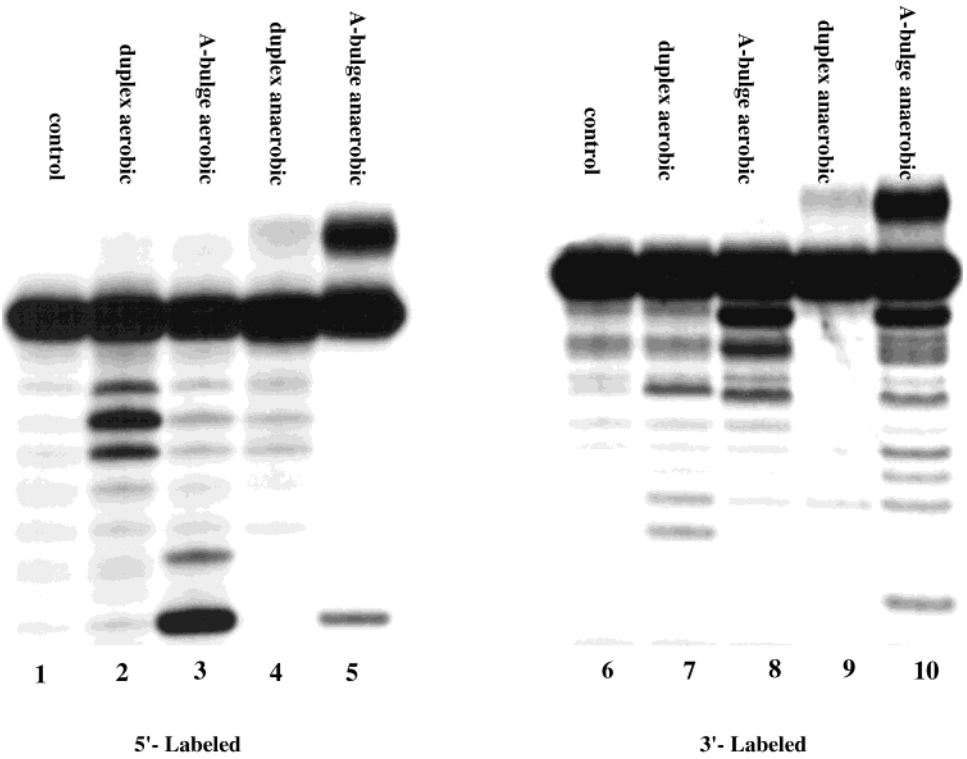

FIGURE 7: Covalent drug−DNA adduct formation under anaerobic conditions. Reactions of thiol-activated NCS-chrom with duplexes of 5′ end-(lanes 1−5) or 3′ end-(lanes 6−10) labeled D_1 and complementary D_{1-0} or D_{1-10} were performed under aerobic (lanes 2, 3 and 7, 8) or anaerobic (lanes 4, 5 and 9, 10) conditions. Lanes 1 and 6, control lanes without drug.

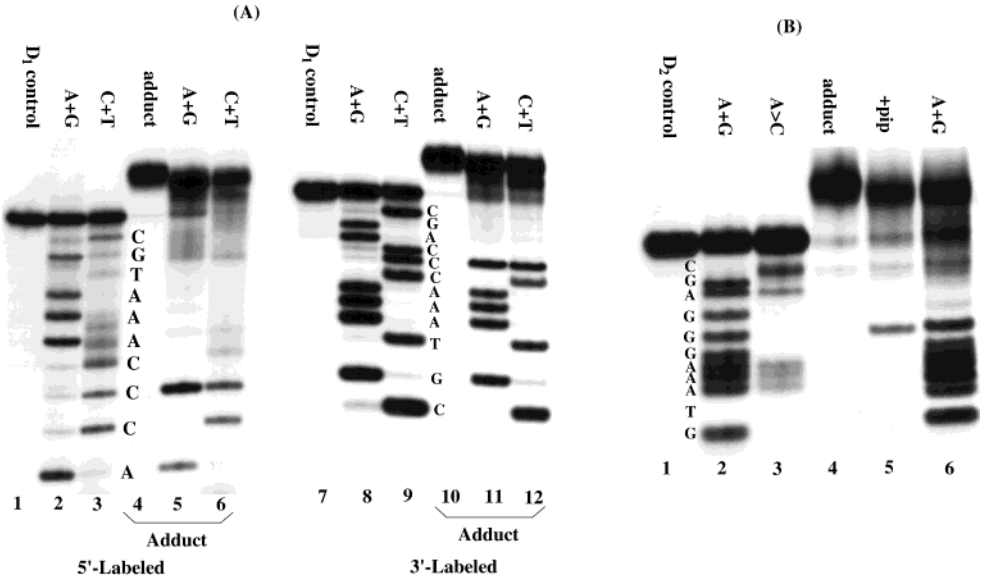

FIGURE 8: DNA site of attachment of covalent adduct. (A) Chemical sequencing was carried out to determine the drug attachment site on D_1. The samples were isolated from lanes 5 and 10 of Figure 7. Lanes 1−6, 5′ end-labeled samples; lanes 7−12, 3′ end-labeled samples. Lanes 1 and 7 controls for D_1; lanes 4 and 10, controls for adduct without any treatment. Lanes 2, 3 and 8, 9, sequencing lanes for D_1; lanes 5, 6 and 11, 12, chemical sequencing lanes for the adduct. (B) Piperidine treatment and A+G reaction of the adduct formed with D_2 and D_{2-1} duplex. D_2 was 3′ end-labeled. Lanes 1−3, control and sequencing lanes of D_2; lane 4, reisolation of the adduct from the reaction of the drug with the duplex of D_2 and D_{2-1} under anaerobic reactions; lane 5, treatment of the adduct (lane 4) with piperidine at 90 °C for 30 min leads to a strand break at the G(5) position; lane 6, A + G reaction for the adduct.

the highest cleavage efficiency, the K_d is little different from that for bulges containing pyrimidines. Similarly, the bulge with two adenine bases has a K_d value close to that of single A base bulge, although there is a large difference between them in term of cleavage (Tables 1 and 2). The cleavage of the hairpin duplexes was also examined, and the results show a pattern similar to the duplexes formed by two separate strands. Among the four oligonucleotides tested, the adenine base bulge gives the strongest cleavage with a selectivity index of 8, and the other three bulges have a selectivity index of 0.7 (AA) and about 2.5 (C and CC) (Table 3).

A possible explanation for the difference between the binding and cleavage data is that the cleavage efficiencies are to a large extent controlled kinetically instead of thermodynamically. In considering the cleavage data, two important issues associated with efficient cleavage need to

Scheme 3: Possible Rationale for the Strand Scission of the Adduct Strand upon Piperidine Treatment

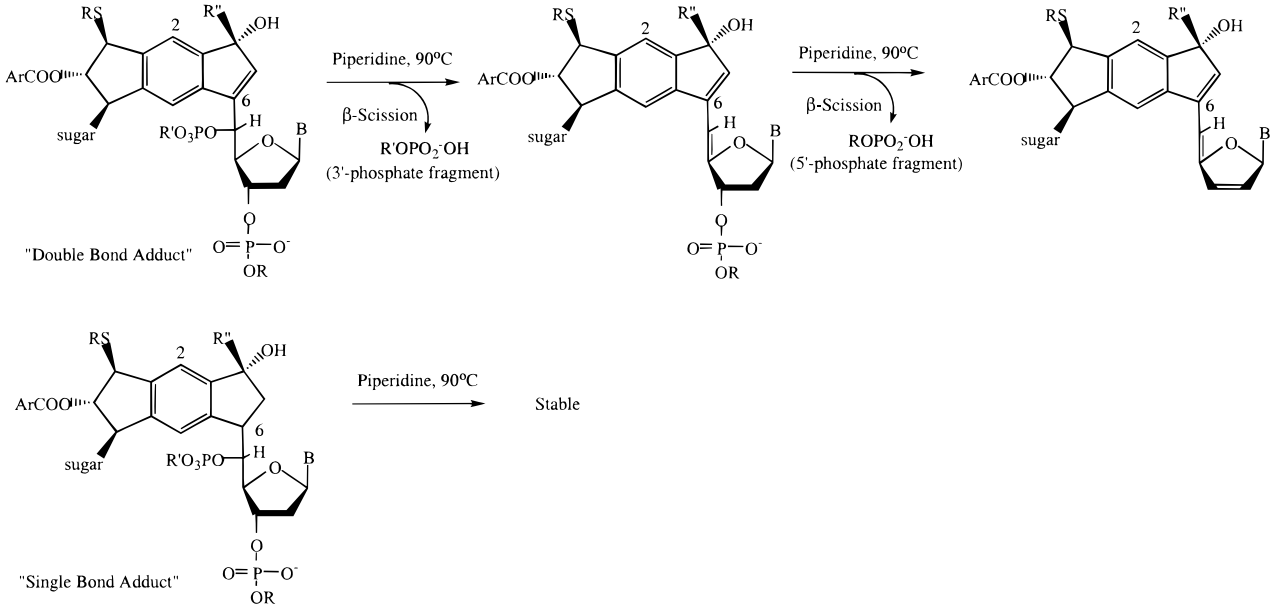

be considered. One is how strongly the NCS chromophore preferentially binds to the bulge site (thermodynamic factor), and the other is how efficiently the radical can abstract hydrogen from the deoxyribose (kinetic factor, based on stereochemical considerations). The actual cleavage data reflect the combination of these two factors. The relatively lower selectivity in binding and high selectivity in cleavage indicate that the kinetic factor must be playing the major role during the reaction and likely reflect the geometry of the complex involved in hydrogen abstraction (vide supra).

Covalent Adduct: Formation, Sequencing, and Alkaline Instability. Dioxygen is required for the carbon-centered sugar radicals to undergo oxidative degradation to generate the 5′ aldehyde and 3′ phosphate fragments as the final products. Under anaerobic conditions, reactions of duplex DNAs with NCS-chrom lead to the formation of a covalent adduct on the nucleic acid sugar, as detected as a band moving more slowly on electrophoresis than the parent DNA. Adduct formation has been observed with normal duplex DNA (*42*), with DNA bulges under base-catalyzed conditions (in the absence of thiol) (*43*) and with a DNA−RNA hybrid having a RNA overhang (*44*). As shown here (Figure 7), an adduct is also formed in the reaction with thiol-activated chromophore and bulged DNAs, when oxygen is excluded from the reaction. Lanes 4, 5, 9, and 10 are the results from reactions under anaerobic conditions with annealed D_1 and D_{1-0} and D_1 and D_{1-10}. The target strand D_1 was labeled at the 5′ (lanes 1−5) or 3′ (lanes 6−10) end. A significant amount of slow-moving band material, which is presumably adduct, was formed from the reaction involving an A bulge (lanes 5 and 10), whereas adduct formation (presumably at the T site) in pure duplex DNA is hardly seen under these conditions (lanes 4 and 9). Further, there was no adduct formation on the bulge strand under anaerobic conditions (data not shown). The slow-moving bands from lanes 5 and 10 were excised and purified, and chemical sequencing methods were used to determine the drug attachment site.

Maxam and Gilbert sequencing (A + G and C + T) was employed in an effort to identify the covalent linkage site of the adduct on the DNA (Figure 8A). Analysis of the cleavage products from both 3′ end-labeled and 5′ end-labeled D_1 reveals that the attachment site for the drug is at the C(5) position, which is the same location where cleavage occurs under aerobic conditions. This conclusion was based on comparison of the sequencing cleavage bands of the adduct and that of the control lanes (lanes 2, 3 and 8, 9): the base ladder of the fragments from the adduct matches the bands on the control lanes only for fragments shorter than C(5).

Unexpectedly, with the adduct sample, there is also one band on each of the A + G sequencing lanes at the C(5) positions in both 5′- and 3′-labeled D_1 (lanes 5 and 11, respectively), but not with the duplex sample (lanes 2 and 8), indicating an adduct-associated strand break of the oligonucleotide at the adduct attachment site. Subsequent studies revealed that this band can be induced by a simple piperidine treatment of the adduct sample at 90 °C for 30 min, and the intensity of the band does not increase beyond that found with the A + G treatment upon longer base treatment, despite the continued presence of the original adduct (data not shown). To determine whether this cleavage is cytosine base specific, we examined the adduct generated at the G site. An adduct was also formed from the reaction of annealed D_2 and D_{2-1} with thiol-activated NCS-chrom under anaerobic conditions (the 3′ end of D_2 was labeled), and this adduct was separated and sequenced (Figure 8B). As shown in lanes 2 and 6, it is obvious that the drug is attached to the G(5) position of D_2, and it also generates a strand break at this position when the adduct is treated with piperidine (lane 5), indicating that the adduct-associated strand scission is not base specific. As expected for an adduct on the deoxyribose chain, there is no difference in the scission behavior between purine and pyrimidine bases.

The partial strand breakage of the isolated adduct band at the attachment site by piperidine treatment is interesting and indicates that the adduct formed under these reaction conditions is actually a mixture of at least two types. Part (~10%) is alkali-labile, and the rest is stable to alkaline treatment. The breakdown gives either a fragment with a 5′ phosphate for 5′ end-labeled D_1 or a fragment with a 3′

phosphate for 3′ end-labeled D_1, as judged by their identical mobilities as corresponding chemical sequencing bands. It is plausible that the two species of drug−DNA adduct come from the same biradical drug intermediate, through the addition of the newly generated 5′ carbon deoxyribose radical to the double bond involving the newly quenched C6 radical of the drug. This would lead to either an adduct containing a single-bond between C5 and C6 (single bond adduct) or to one containing a double-bond between C5 and C6 (double bond adduct). The latter could also come from radical collision between the newly formed C5′ radical and the second incoming biradical drug intermediate. The double-bond adduct would be expected to be base-labile and lead to the breakage of the nucleotide chain upon reacting with hot piperidine by two successive β-scissions, forming both the 3′ phosphate and 5′ phosphate-ended fragments (Scheme 3). We expect that structure determination of these drug adducts will shed further light on the precise mechanism of this type of DNA damage.

REFERENCES

1. Xi, Z., and Goldberg, I. H. (1999) in *Comprehensive Natural Products Chemistry* (Barton, D. H. R., and Nakanishi, K., Eds.) Vol. 7, pp 553−592, Elsevier Science, Oxford.
2. Goldberg, I. H., Kappen, L. S., Xu, Y. J., Stassinopoulos, A., Zeng, X., Xi, Z., and Yang, C. F. (1996) *DNA and RNA Cleavers and Chemotherapy of Cancer and Viral Diseases*, pp 1−21, Kluwer Academic, Netherlands.
3. Goldberg, I. H., and Kappen, L. S. (1995) in *Enediyne Antibiotics as Antitumor Agents* (Borders, D. B., and Doyle, T. W., Eds.) pp 327−362, Dekker, New York.
4. Goldberg, I. H. (1991) *Acc. Chem. Res.* 24, 191−196
5. Dasgupta, D., and Goldberg, I. H. (1985) *Biochemistry* 24, 6913−6920.
6. Myers, A. G. (1987) *Tetrahedron Lett. 28*, 4493−4496.
7. Gao, X., Stassinopoulos, A., Rice, J. S., and Goldberg, I. H. (1995) *Biochemistry 34*, 40−49.
8. Gao, X., Stassinopoulos, A., Gu, J., and Goldberg, I. H. (1995) *Bioorg. Med. Chem. 3*, 795−809.
9. Kappen, L. S., and Goldberg, I. H. (1993) *Science 261*, 1319−1321.
10. Kappen, L. S, and Goldberg, I. H. (1993) *Biochemistry 32*, 13138−13145.
11. Hensens, O. D., Zink, D. L., Chin, D.-H., Stassinopoulos, A., Kappen, L. S., and Goldberg, I. H. (1994) *Proc. Natl. Acad. Sci. U.S.A. 91*, 4534−4538.
12. Stassinopoulos, A., Ji, J., Gao, X., and Goldberg, I. H. (1996) *Science 272*, 1943−1946.
13. Xi, Z., Mao, Q. K., and Goldberg, I. H. (1999) *Biochemistry 38*, 4342−4354.
14. Turner, D. H. (1992) *Curr. Opin. Struct. Biol. 2*, 334−337.
15. Lilley, D. M. (1995) *Proc. Natl. Acad. Sci. U.S.A. 92*, 7140−7142.
16. Chastain, M., and Tinoco, I., Jr. (1991) *Progress in Nucleic Acid Research and Molecular Biology*, Vol. 41, pp 131−177, Academic Press, New York.
17. Ripley, L. S. (1982) *Proc. Natl. Acad. Sci. U.S.A. 79*, 4128−4132.
18. Streisinger, G., Okada, Y., Emrich, J., Newton, J., Tsugita, A., Terzaghi, I., and Inouye, M. (1966*) Cold Spring Harbor Symp. Quantum Biol. 31*, 77−84.
19. Kunkel, T. A. (1993) *Nature* 365, 207−209.
20. Malkov, V. A, Biswas, I., Camerini-Otero, R. D., and Hsieh, P. (1997) *J. Biol. Chem. 272*, 23811−23817.
21. Wang, Y.-H., Bortner, C. D., and Griffith, J. (1993) *J. Biol. Chem. 268*, 17571−17577.
22. Ashley, C. T., Jr., and Warren, S. T. (1995) *Annu. Rev. Genet. 29*, 703−728.
23. Kalnik, M. W., Norman, D. G., Li, B. F., Swann, P. F., and Patel, D. J. (1990) *J. Biol. Chem. 265*, 636−647.
24. Aboul-Ela, F., Murchie, A. I. H., Homans, S. W., and Lilley, D. M. (1993) *J. Mol. Biol. 229*, 173−188.
25. Dornberger, U., Hillisch, A., Gollmick, F. A., Fritzsche, H., and Diekmann, S. (1999) *Biochemistry 38*, 12860−12868.
26. Leblanc, D. A., Morden, K. M. (1991) *Biochemistry 30*, 4042−4047.
27. Ricce, J. A., and Crothers, D. M. (1989) *Biochemistry 28*, 4512−4516.
28. Nelson, J. W., and Tinoco, I., Jr. (1985) *Biochemistry 24*, 6416−6421
29. White, S. A., and Draper, D. E. (1987) *Nucleic Acids Res. 15*, 4049−4064.
30. Yao, S., and Wilson, W. D. (1992) *J. Biomol. Struct. Dyn. 10*, 367−387.
31. Williams, L. D., and Goldberg, I. H. (1988) *Biochemistry 27*, 3004−3011.
32. Williams, L. D., and Goldberg, I. H. (1988) *Nucleic Acids Res. 16*, 11607−11615.
33. Myers, A. G., Cohen, S. B., and Kwon, B.-M. (1994) *J. Am. Chem. Soc. 116*, 1670−1682.
34. Kappen, L. S., and Goldberg, I. H. (1985) *Nucleic Acids Res. 13*, 1637−1648.
35. Maxam, A., Gilbert, W. (1977) *Proc. Natl. Acad. Sci. U.S.A. 74*, 560−564.
36. Xi, Z., Jones, G. B., Qabaja, G., Wright, J., Johnson, F., and Goldberg, I. H. (1999) *Org. Lett. 1*, 1375−1377.
37. Kusakabe, T., Uesugi, M., and Sugiura, Y. (1995) *Biochemistry 34*, 9944−9950.
38. Zeng, X., Xi, Z., Kappen, L. S., Tan, W., and Goldberg, I. H. (1997) *Biochemistry 36*, 14975−14984.
39. Kappen, L. S., Goldberg, I. H. (1995) *Biochemistry 34*, 5997−6002.
40. Kappen, L. S., Xi, Z., and Goldberg, I. H. (1997) *Bioorg. Med. Chem. 5*, 1221−1227.
41. Stassinopoulos, A., and Goldberg, I. H. (1995) *Bioorg. Med. Chem. 3*, 713−721.
42. Povirk, L. F., and Goldberg, I. H. (1985) *Biochemistry 24*, 4035−4040.
43. Kappen, L. S., and Goldberg, I. H. (1997) *Biochemistry 36*, 14861−14867.
44. Zheng, P., Liu, C., Xi, Z., Smith, R. D., and Goldberg, I. H. (1998) *Biochemistry 37*, 1706−1713.

BI000007T